REPORT
doi:10.26443/seismica.v5i1.2999

SEISMICA

A rare earthquake in the upper mantle of subcontinental lithospheric mantle of North America

Benedict Fitton * [1], **Timothy J. Craig** [1], **Sebastian Rost** [2]

[1]COMET, School of Earth, Environment and Sustainability, University of Leeds, Leeds, LS2 9JT, UK, [2]School of Earth, Environment and Sustainability, University of Leeds, Leeds, LS2 9JT, UK

Author contributions: *Conceptualization*: Benedict Fitton, Timothy J. Craig. *Methodology*: Benedict Fitton. *Formal Analysis*: Benedict Fitton. *Investigation*: Benedict Fitton. *Writing - Original draft*: Benedict Fitton. *Writing - Review & Editing*: Timothy J. Craig, Sebastian Rost. *Visualization*: Benedict Fitton. *Supervision*: Sebastian Rost, Timothy J. Craig. *Project administration*: Timothy J. Craig. *Funding acquisition*: Timothy J. Craig.

Abstract Earthquakes occurring in stable continental mantle lithosphere are extremely rare, with a small number of cases restricted to northern Australia, the India-Asia collision zone, and western North America. Here, we use a combination of regional seismic waveform modelling and teleseismic array data to confirm the location of a small (M_w 4.1) earthquake from September 2025 under northern Utah, whose depth places it firmly below the local Moho, and into the continental mantle. This joins other reported small-magnitude seismicity under the eastern Rocky Mountains, principally in Utah and Wyoming, who's causative mechanism remains enigmatic. The focal mechanism of this earthquake is consistent with those of other reported mantle seismicity, but contrasts with the shallower crustal stress field, indicating that seismicity in the mantle in this region may not reflect the shallow crustal geodynamics of the region, and is unlikely to be playing a role in supporting long-term stresses.

Non-technical summary Earthquakes in the continental mantle are extremely rare, with only a few confirmed examples. Here, we add another to this confirmed list of continental mantle earthquakes, with a M_w 4.1 earthquake under northern Utah in 2025. The processes allowing brittle seismogenic failure to happen at such depths remain uncertain.

Production Editor:
Kiran Kumar Thingbaijam
Handling Editor:
Ryo Okuwaki
Copy & Layout Editor:
Théa Ragon

Received:
April 10, 2026
Accepted:
May 28, 2026
Published:
June 3rd, 2026

1 Introduction

Earthquakes that rupture within the continental lithospheric mantle are rare. Documented examples include events beneath the Arafura Sea north of Australia (Sloan and Jackson, 2012), the South Indian Shield (Paul et al., 2025), and in western North America (Zandt and Richins, 1979; Craig and Heyburn, 2015; Frohlich et al., 2015; Woo and Chen, 2025; Hutchings et al., 2025, 2026). There is also the more contentious case of deep seismicity beneath the Himalayas and across western and southern Tibet, where deep (~70 - 90 km) earthquakes have been interpreted either as occurring sub-Moho in the uppermost mantle or within a thickened seismogenic lower crust (Chen and Molnar, 1983; Monsalve et al., 2006; Priestley et al., 2008; Schulte-Pelkum et al., 2019; Craig et al., 2020, 2023). The case of the Himalayas/Tibet highlights the challenge of designating earthquakes as sub-Moho when focal depth and Moho depth are both uncertain.

At 23:57:47 on 10 September 2025 a M_w 4.1 earthquake was reported beneath northern Utah. The epicentre is located ~360 km SW of the Wyoming Craton and ~450 km SE of the Yellowstone hotspot (Figure 1a). The southwest edge of the Wyoming Craton has been interpreted as an area of elevated strain, linked to a strong lateral gradient in temperature, and has been associated with a seismogenic region of lithospheric mantle, manifest through sparse, low-magnitude mantle seismicity (Hutchings et al., 2025). The Yellowstone hotspot has been associated with episodes of mantle upwelling and lithospheric delamination, with the adjacent Snake River Plain (SRP, which marks out the hotspot path) recording ~17 Myr of plume-related volcanism (Hanan et al., 2008). Rigo et al. (2015) interpret a regional crustal stress field that is NE-SW extensional north of the SRP and E-W extensional south of the SRP, a conclusion supported by the orientation of crustal earthquake focal mechanisms and GPS velocity data. Previous studies have suggested that continental mantle earthquakes may reflect the same regional stress field orientations observed in the crust (Hutchings et al., 2025), raising questions about the relationship between crustal and lithospheric mantle strength, and the potential for coherent deformation and the support of stress across a broad depth range of the lithosphere.

The very occurrence of continental mantle seismicity remains enigmatic, with such earthquakes occurring at depths usually incapable of seismogenesis through Mohr-Coulomb brittle failure. Four different mechanisms have been proposed to explain continental mantle seismicity: (a) standard Mohr-Coulomb failure operating in cold mantle lithosphere, requiring very high stresses; (b) dehydration-related embrittlement, re-

*Corresponding author: ed20bjcf@leeds.ac.uk

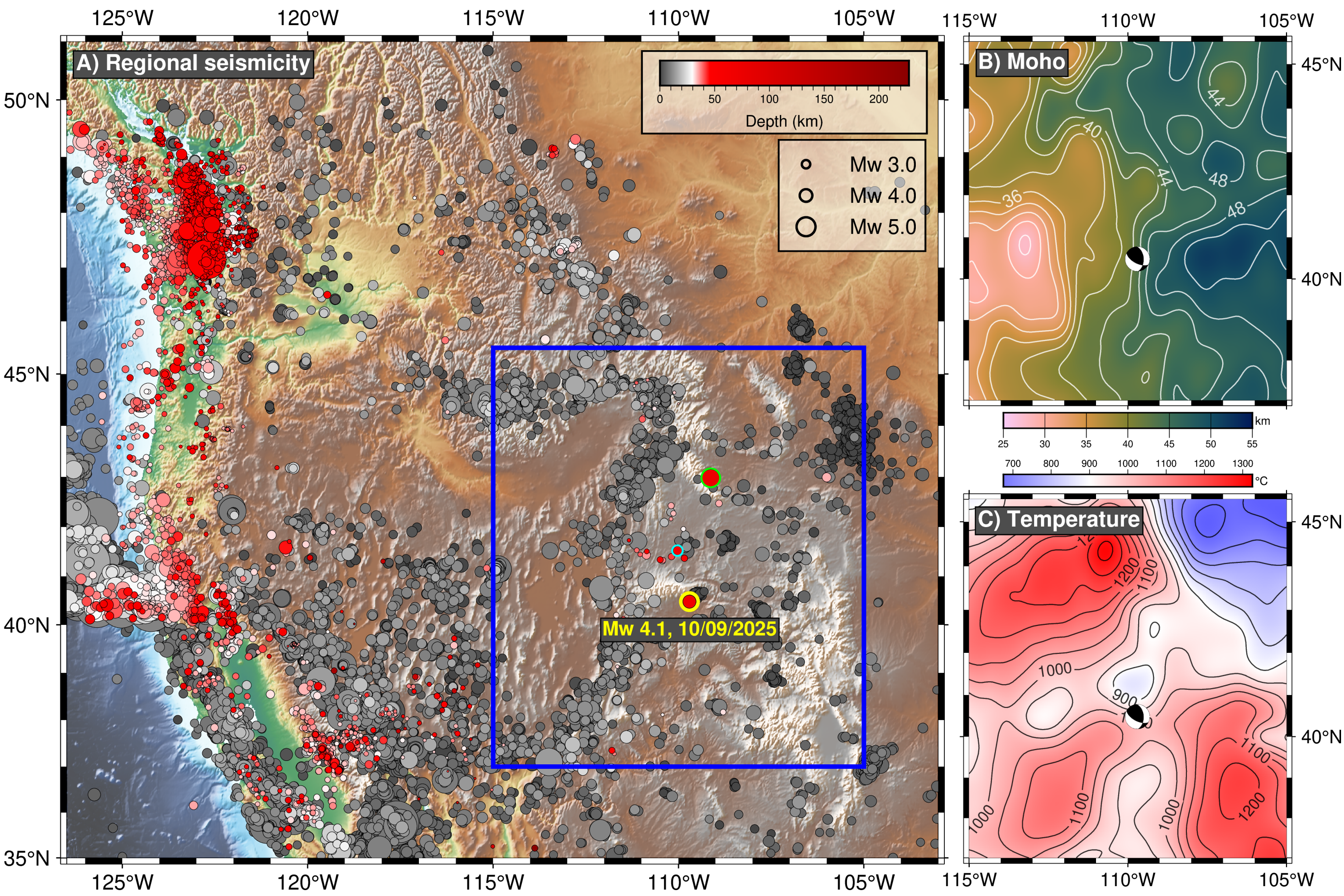

Figure 1 A) Regional seismicity plotted over topography for western North America. Earthquakes shallower than 30 km include only events where $M_w \geq 3.0$; all earthquakes deeper than 30 km are shown. Earthquakes are colour-coded by hypocentral depth and scaled by magnitude. The 10/09/2025 Utah earthquake is highlighted with a yellow ring. The M_l 3.2 2019 Granger earthquake is highlighted with a cyan ring. The M_w 4.7 2013 Wind River earthquake is highlighted with a green ring. The Earthquake locations are taken from the USGS earthquake catalogue (USGS, 2017). B) Depth to the Moho (km) (from the surface) taken from McCafferty et al. (2023), with 2 km contours. The focal mechanism of the Utah earthquake is plotted at its epicentral location. C) Temperature (°C) at 60 km depth taken from Shinevar et al. (2023) with 50°C contours. The focal mechanism is again plotted at its epicentral location.

quiring that the surrounding material is undergoing changes in pressure and temperature sufficient to lead to petrological evolution, and dehydration; (c) shear-heating, leading to an initially viscous process dropping the yield stress of the fault zone, progressing into brittle failure; (d) high-strain-rate and high stress deformation of material usually too hot to fail seismogenically, typically related to fluid migration.

Sparse small-magnitude mantle earthquakes ($M < 2.5$) beneath the Ruwenzori mountains of Uganda and the Democratic Republic of the Congo, in the Western Branch of the East African Rift system, have been attributed to rapid magma ascent and associated transient stresses (Lindenfeld and Rümpker, 2011), with high localised stresses and rapid strain rates enabling brittle failure. Similar mechanisms have been invoked to explain surprising lower crustal seismicity in hot, active deformation zones in New Zealand (Reyners et al., 2007), and Iceland Soosalu et al. (2010). However, mantle earthquakes in western North America are well-described by a double-couple moment tensor and appear to lack a significant isotropic component (Craig and Heyburn, 2015; Frohlich et al., 2015, this study), indicating an absence of volumetric sources often associated with magmatic intrusion.

Mantle seismicity in the Arafura sea has been located in colder regions of the lithospheric mantle, at temperatures below 600 °C - sufficiently cold for brittle failure (Sloan and Jackson, 2012). Similarly, rare seismicity just below the Moho of peninsular India, south of the Himalayas, typically happens in old, cold lithosphere where the uppermost mantle is likely cold enough to allow simple brittle failure (Craig et al., 2012; Paul et al., 2025). Previous mantle seismicity under western North America has been reported substantially below the Moho, at depths where failure in anomalously cold mantle lithosphere is unlikely to be the cause (Craig and Heyburn, 2015; Prieto et al., 2017; Hutchings et al., 2025).

Both shear heating and dehydration related processes remain in contention for mechanisms to explain the occurrence of mantle seismicity under western North America, with different studies having argued either process can explain the ~75 km-deep 2013 M_w 4.7 Wind River earthquake (Figure 1) under Wyoming – the largest, and best studied of the reported mantle earth-

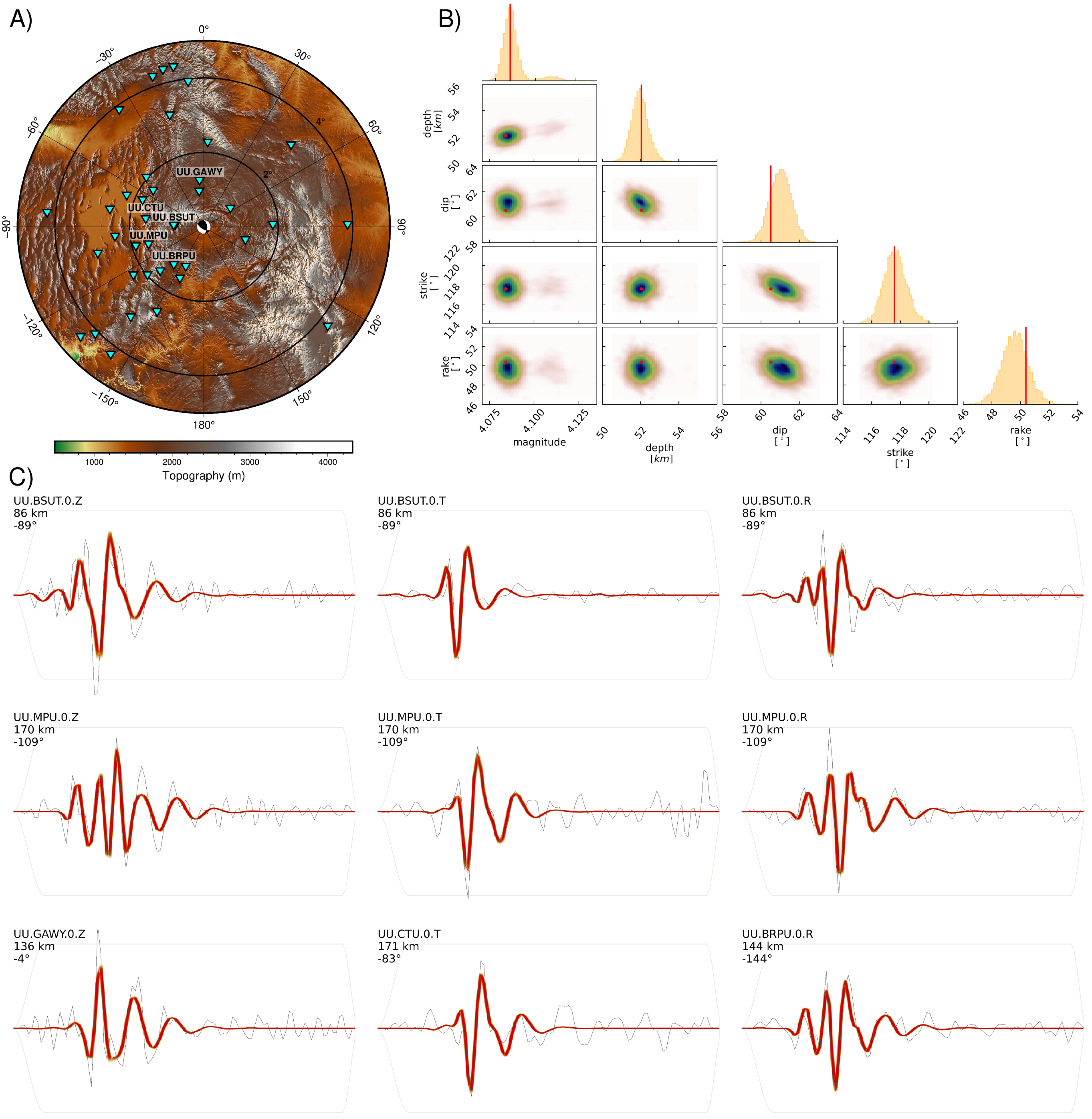

Figure 2 A) Map of the stations used for the regional waveform inversion with the stations from which waveforms are taken for Figure 2C labelled. The focal mechanism of the 10/09/2025 Utah earthquake plotted at the centre. Thick lines show epicentral distance every 2°. B) Correlation histograms from the regional waveform inversion, showing the posterior distribution of earthquake source parameters. The preferred, minimum misfit solution is highlighted in red. C) Waveform fits for a subset of stations. Waveform fits for all stations can be found in supplementary material. Black traces show observed waveforms and red traces show the synthetic waveforms of the 100 best-fitting solutions. Each trace is labelled with network, station, and component, then epicentral distance (km) and event-to-station azimuth (°).

quakes. Prieto et al. (2017) suggested that this earthquake occurred as a result of shear heating and thermal runaway in material too hot to otherwise fail seismogenically – a conclusion supported by the isolated nature of this earthquake, with only a single aftershock reported (Craig and Heyburn, 2015; Thielmann, 2018). In contrast, both Li and Dave (2016) and Zhao et al. (2024) advocate for a role for the deeper Farallon slab in the deeper mantle beneath North America, either through driving small-scale mantle convection at the edge of Wyoming Craton, with erosion of the craton edge facilitated by hydration of the cratonic root by fluids released by the remnant Farallon slab, or more directly, with seismicity in the lithospheric mantle being permitted by dehydration embrittlement during the passage of fluids expelled from the descending slab.

Potentially distinguishing between these different drivers requires a detailed understanding of how these earthquakes fit into their regional geodynamic context, precise source locations, and detailed seismological analysis of their source processes. However, most confirmed continental mantle earthquakes are small (M_w < 4). In North America, the largest documented continental lithospheric mantle earthquake is M_w 4.7 (Wind River, 2013; Frohlich et al., 2015; Craig and Heyburn, 2015; Prieto et al., 2017). The small magnitudes of most of the reported events limit signal-to-noise ratios, making it difficult to recover accurate hypocentral depths and focal mechanisms. Hutchings et al. (2026) produced a composite focal mechanism to characterise a cluster of mantle earthquakes beneath Alberta because individual events were too small. Recent work by Woo and Chen (2025) identified additional small mantle earthquakes beneath the Wyoming Craton, including an M_L 1.4 event in 2020 located close to the 2025 M_w 4.1 Utah earthquake.

Here we present a seismological investigation of a M_w 4.1 earthquake beneath northeastern Utah (Figure 1), reported at a depth of 68 km by the NEIC (USGS, 2017) and 72 km by the IDC (Arora et al., 2012). We carry out a regional waveform inversion to determine a focal mechanism and revise centroid depth. We obtain independent constraints from teleseismic depth-phase analysis. This event provides a valuable new data point in the small but growing catalogue of continental mantle earthquakes in North America.

2 Data and Methods

2.1 Regional waveform inversion

For an initial regional waveform solution, we use waveform data from 39 stations within a 5° radius of the earthquake epicentre (Figure 2A). Waveforms are bandpass filtered between 0.04 - 0.09 Hz, and rotated into transverse and radial components based on the initial earthquake location. We select a total of 36 vertical, 9 transverse, and 7 radial components in which signal could be identified above background noise (Figure S1), noting that the predominance of the vertical component is initially consistent with the reduced amplitude of the surface waves, as would be expected for a sub-Moho earthquake with a deep centroid. We perform a probabilistic regional waveform inversion using the Bayesian Earthquake Analysis Tool (BEAT; Vasyura-Bathke et al., 2019), assuming a pure double-couple source. Green's functions are computed using the AK135 1-D velocity model modified using CRUST 2.0 (Bassin, 2000) to incorporate the regional crustal structure. We invert a 100 s time window around main body-wave arrivals, synthetic waveforms are realigned against observed waveforms using cross-correlation at each iteration, as mechanism for correcting for any timing errors or overall travel-time uncertainties. We assign greater weight to the vertical component waveforms because they more consistently showed good signal-to-noise ratios. We use BEAT's L2-norm waveform misfit and Markov-Chain Monte-Carlo sampling scheme. This approach allows for the setting of appropriate priors and provides posterior distributions, giving confidence that our solution reflects a well-constrained region of model space.

The inversion yields well-constrained focal mechanisms showing oblique thrust faulting. The best-fitting solution has a strike of 118°, a dip of 60°, a rake of 50°, and a magnitude of approximately M_w 4.1 (Figure 2B). We find a revised focal depth of 52 km, 16 km shallower than the initial NEIC estimate. The posterior distributions give us confidence that the mechanism and depth are well resolved, and our revised depth gives us confidence that the event is sub-Moho.

2.2 Teleseismic depth-phase analysis

Whilst routine catalogues are known to lack the fine-scale resolution, particularly in depth, for reliably determining which side of the Moho a candidate mantle earthquake may be on (Craig et al., 2023), a ∼16 km depth difference to the NEIC preferred solution is perhaps more substantial than might be expected. To provide independent depth constraint, we analyse *P*, *pP*, and *sP* arrivals recorded at eight small aperture seismic arrays located between 30° and 90° epicentral distance (teleseismic distance, Figure 3). We also processed data from the Yellowknife array (Figure S2), but, due to the proximity of this array to the earthquake (22.2°) interpretation of the resulting waveforms was complicated by its position within the upper mantle triplication zone.

For each array, we first estimate the optimal slowness vector of the incoming *P* wave. This is done using an Nth-root stacking approach (N = 2) (Rost and Thomas, 2002), computing power within a ±10-s window around the predicted *P* arrival time, with predicted arrival times calculated using the AK135 1-D velocity model. To avoid convergence on local maxima, optimisation is performed in two stages: (1) a coarse grid search over slowness space, followed by (2) a refinement of the best 12 candidate solutions using a Nelder–Mead search. The optimal slowness vector obtained from the nth-root beamforming search is then applied to the original (un-rooted) traces, which are time-shifted accordingly and linearly stacked to produce a beamformed trace for each array (Figure 3). We also compute vespagrams with one component of slowness fixed and the other allowed to vary over a range of ± 0.2 s/km (Figure 3).

We compute theoretical radiation patterns for the *pP* and *sP* depth phases from our preferred regional waveform solution (Figure 2). The radiation patterns show that all eight arrays lie in a region of low predicted *pP* amplitude and high predicted *sP* amplitude, which is consistent with the phases we observe in the beamformed traces (Figure 3). We also consider *pmP*, the underside-Moho reflection; however, while some traces might include *pmP*, the evidence is not coherent enough to support a confident interpretation (Figure S2). Data from other small-aperture arrays at teleseis-

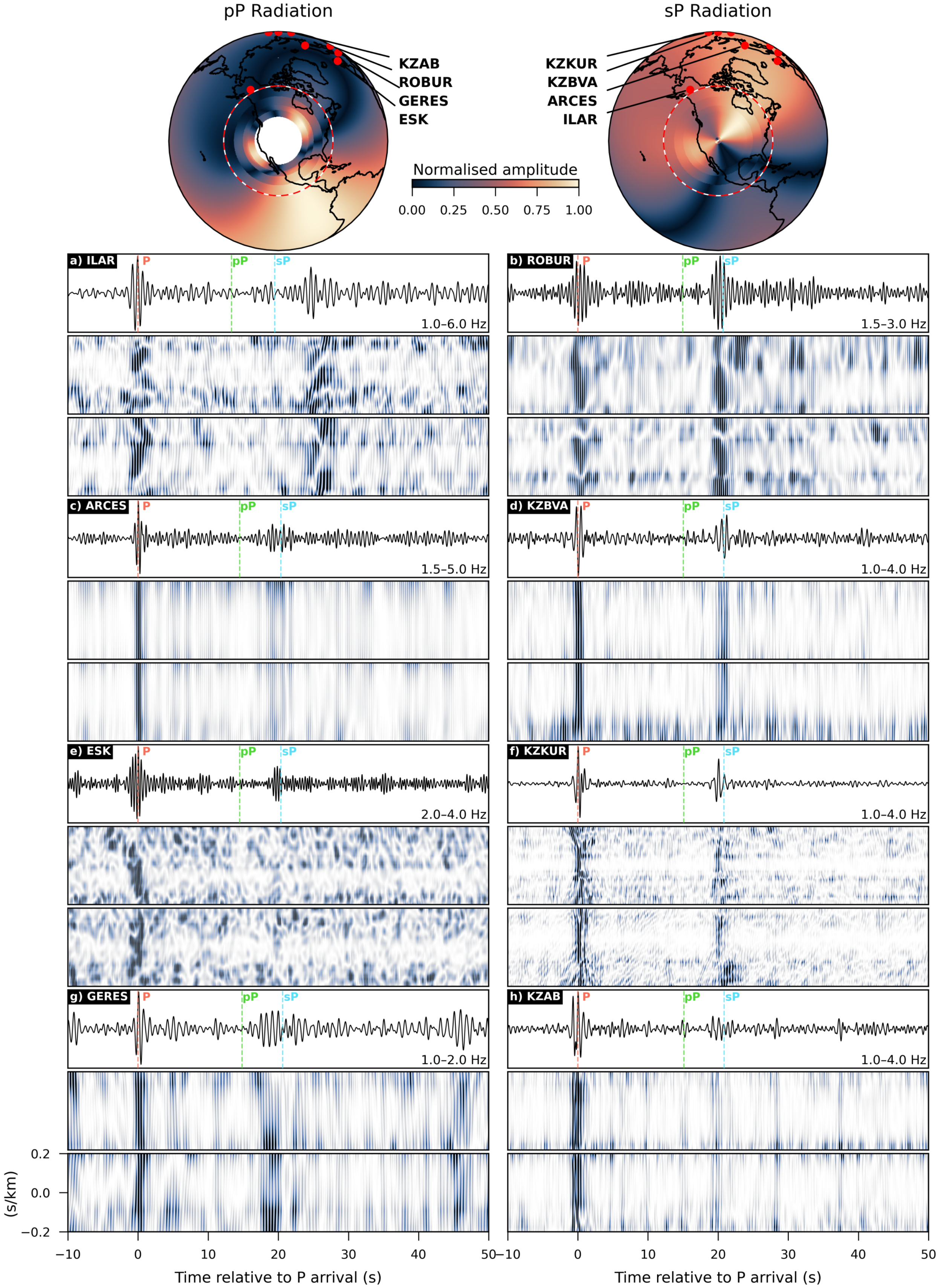

Figure 3 The top panels show theoretical radiation patterns for the phases *pP* and *sP* from the M_w 4.1 2025 Utah earthquake. Colour indicates normalised amplitude of the predicted wavefield. The locations of the teleseismic arrays used in this study are plotted as red dots. A red and white ring marks 30° epicentral distance. Panels (a-h) each correspond to one teleseismic array and contain a beamformed trace followed by two vespagrams. The beamformed trace is computed as described in section 2.2, with predicted arrival times for *P* (orange), *pP* (green), and *sP* (blue) marked. In the upper vespagrams, Sy is fixed and Sx is allowed to vary; in the lower vespagrams, Sx is maintained and Sy is allowed to vary.

mic distances were also processed, but failed to yield clear, coherent signals above the noise level – consistent with the low predicted amplitudes of arrays in other geographic locations, based on the predicted radiation pattern.

Teleseismic depth-phase analysis supports the focal depth obtained through the regional waveform inversion. Clear *P*-wave arrivals are identified at all eight arrays and, as predicted by the theoretical radiation patterns, the *sP* phase is consistently more prominent than the *pP* phase. The delay from *P* to *sP* provides support for a focal depth of ∼52 km, indicating a source region in the uppermost lithospheric mantle, somewhat shallower than the 2013 Wind River event.

3 Discussion and Conclusion

Regional waveform inversion, supported with teleseismic depth-phase analysis, shows the M_w 4.1 2025 Utah earthquake ruptured at a depth of ∼52 km. Koper et al. (2026) reported a focal depth of ∼60–70 km for the same event. This discrepancy may reflect differences in data selection, station distribution, and velocity models. Our depth estimate is supported by teleseismic beamforming, which provides additional constraints on depth-sensitive phases that were not exploited in Koper et al. (2026). Theoretical radiation patterns indicate that the dominant teleseismic depth phase is *sP* rather than *pP*, and the alignment between observed and predicted *sP* arrivals supports a shallower depth in our preferred range (Figure 3). Both studies place the earthquake sub-Moho, and the inferred focal mechanisms are highly consistent (Kagan angle = 7.5°; Tape and Tape, 2012). Moho depths in this region are well constrained thanks to extensive imaging using USArray Transportable Array (TA) data, including receiver-function, surface-wave, and travel time tomography studies (Kind et al., 2012; Shen and Ritzwoller, 2016; Zhang et al., 2020; Xiao et al., 2025). In Figure 1 we show depth to Moho from the surface (McCafferty et al., 2023) and estimated temperature at 60 km depth (Shinevar et al., 2022). As these maps show, the Moho in this region is estimated to be at ∼44 km, and we are therefore confident that the revised focal depth of ∼52 km is sub-Moho. Similarly, wavespeed-based temperature estimation suggests that temperatures reach ∼900 °C only marginally below our estimated source depth, indicating that the earthquake ruptured at higher temperatures than would typically be expected for brittle failure (Figure 1C).

In comparison to other continental lithospheric mantle seismicity, the North American situation seems unique. The mantle seismicity observed beneath the Arafura Sea and beneath the Himalaya/Tibet occurs in anomalously cold lithospheric mantle (Sloan and Jackson, 2012; Craig et al., 2012). This is not the case in western North America. Beneath the East African Rift and beneath Iceland and New Zealand, mantle seismicity is associated with magma impregnation, again this is not something that can reasonably be expected in western North America.

In the context of other North American continental mantle seismicity, the M_w 4.1 2025 Utah earthquake is the second largest recorded after the M_w 4.7 2013 Wind River earthquake. The focal mechanism from this study is only the second well-constrained example for this type of event in this region. The 2025 Utah earthquake shares several features with the M_w 4.7 2013 Wind River earthquake. Both exhibit thrust-faulting components and, although the Wind River earthquake is more oblique, each shows a significant strike-slip contribution. In both cases, the source is well described by a purely double-couple mechanism, without requiring an isotropic or CLVD component; for the 2025 Utah earthquake, this is consistent with the favoured USGS solution provided by the University of Utah, which finds a 99% double-couple source (USGS, 2017). This, as well as the absence of an associated earthquake cluster or aftershock sequence, makes seismogenesis due to magmatic impregnation of the lithosphere unlikely in the case of the M_w 4.1 2025 Utah earthquake (Figure 1A). We also consider fluid migration-related mechanisms unlikely due to the relatively large distance between the earthquake and the Yellowstone hotspot.

The crustal regional stress field south of the Eastern Snake River Plain has been interpreted as E-W extensional (Rigo et al., 2015). The focal mechanism we recover for the Utah event is not consistent with this stress regime: a thrust fault with a strike of 118° implies a compressional principal stress oriented NNE-SSW. Hutchings et al. (2025) argued that the M_w 4.7 2013 Wind River and the composite solution for the M_l 3.2 2019 Granger (Figure 1), Wyoming mantle earthquakes have focal mechanisms which reflect the same stress field as in the crust. We do not observe this in the case of the M_w 4.1 2025 Utah earthquake. This difference in principal stress orientation may reflect heterogeneity or a transition within the mantle stress field, potentially associated with craton-edge dynamics (Koper et al., 2026), or some degree of crust-mantle decoupling.

The most comparable earthquake to the 2025 Utah earthquake is the M_w 4.7 2013 Wind River earthquake. Several mechanisms have been proposed to explain the occurrence of the Wind River earthquake. Prieto et al. (2017) propose that it was triggered by strain localisation in a mantle shear zone. This process may be enhanced by the strong thermal and rheological contrast between the Yellowstone plume and the cold Wyoming Craton, which could drive mantle convection and promote shear localisation at depth. In contrast, Zhao et al. (2024) propose that the 2013 Wind River earthquake may have been induced by ascending fluids derived from the remnant subducted Farallon slab, consistent with high electrical conductivity observed near the edge of the Wyoming Craton (Bedrosian and Frost, 2023). However, the 2025 Utah earthquake appears relatively isolated and there has been no reported aftershock activity, which may argue against a fluid-driven triggering mechanism in this case.

In this study, we have recovered a well-constrained focal mechanism for a rare continental lithospheric mantle earthquake beneath Utah. The solution indicates steeply-dipping, oblique thrusting and implies a NNE-SSW-oriented maximum compressional stress.

We do not draw any strong conclusions about the triggering mechanism, but we do note the geodynamic complexity of the hypocentral location, where convective effects of the Yellowstone hotspot, the remnant Farallon slab, and the edge of the Wyoming Craton all interact. This report demonstrates the utility of combining probabilistic regional waveform inversion and teleseismic depth-phase analysis to constrain earthquake location and focal mechanism. The enigmatic nature of mantle seismicity beneath western North America continues.

Acknowledgements

BF and TJC were supported in this work by the Royal Society under URF\R1\180088, URF\R\231019, and also through COMET, which is the NERC Centre for the Observation and Modelling of Earthquakes, Volcanoes and Tectonics, a partnership between UK Universities and the British Geological Survey.

Data and code availability

All data used in this study are Open Source, available via FDSN. We have used data from the following seismic networks:

Regional Waveform Inversion

UU: University of Utah Regional Seismic Network (22) (University of Utah, 1962),

US: United States National Seismic Network (4) (Albuquerque Seismological Laboratory/USGS, 1990),

IW: Intermountain West Seismic Network (3) (Albuquerque Seismological Laboratory/USGS, 2003),

WY: Yellowstone National Park Seismograph Network (3) (University of Utah, 1983),

C0: Colorado Geological Survey Seismic Network (2) (Colorado Geological Survey, 2016),

N4: Central and Eastern US Network (2) (Albuquerque Seismological Laboratory/USGS, 2013),

IE: INL Seismic Monitoring Program (1) (Idaho National Laboratory, 1972),

RC: BYU-Idaho Network (1) (Brigham Young University-Idaho, 2001),

RE: US Bureau of Reclamation Seismic Networks (1) (1965, no DOI available).

Teleseismic depth-phase analysis:

CN: Canadian National Seismograph Network (YKAR) (Natural Resources Canada, 1975)

GR: German Regional Seismic Network (GERES) (Federal Institute for Geosciences and Natural Resources (BGR), 1976),

II: Global seismograph Network - II (ESK) (EarthScope Consortium, 1986),

IM: International Miscellaneous Stations (ILAR) (Various Institutions, 1965),

KZ: Kazakhstan Network (KZAB, KZBVA, KZKUR) (Institute of Geophysical Research (KNDC), 1994),

NO: NORSAR Station Network (ARCES) (NORSAR, 1971),

RO: Romanian Seismic Network (ROBUR) (National Institute for Earth Physics (NIEP), 1994)

Competing interests

The authors have no competing financial interests.

References

Albuquerque Seismological Laboratory/USGS. United States National Seismic Network. *International Federation of Digital Seismograph Networks*, 1990. doi: 10.7914/SN/US.

Albuquerque Seismological Laboratory/USGS. Intermountain West Seismic Network. *International Federation of Digital Seismograph Networks*, 2003. doi: 10.7914/SN/IW.

Albuquerque Seismological Laboratory/USGS. Central and Eastern US Network. *International Federation of Digital Seismograph Networks*, 2013. doi: 10.7914/SN/N4.

Arora, N. S., Russell, S., and Sudderth, E. NET-VISA: Network Processin Vertically Integrated Seismic Analysis. *Bulletin of the Seismological Society of America*, 103, 2012. doi: 10.1785/0120120107.

Bassin, C. The current limits of resolution for surface wave tomography in North America. *Eos Trans. AGU*, 81:F897, 2000.

Bedrosian, P. A. and Frost, C. D. Geophysical extent of the Wyoming Province, western USA: Insights into ancient subduction and craton stability. *Bulletin*, 135(3-4):725–742, 2023. doi: 10.1130/B36417.1.

Brigham Young University-Idaho. BYU-Idaho Network. *International Federation of Digital Seismograph Networks*, 2001. doi: 10.7914/SN/RC.

Chen, W.-P. and Molnar, P. Focal depths of intracontinental and intraplate earthquakes and their implications for the thermal and mechanical properties of the lithosphere. *Journal of Geophysical Research: Solid Earth*, 88(B5):4183–4214, 1983. doi: 10.1029/JB088iB05p04183.

Colorado Geological Survey. Colorado Geological Survey Seismic Network. *International Federation of Digital Seismograph Networks*, 2016. doi: 10.7914/SN/C0.

Craig, T. and Heyburn, R. An enigmatic earthquake in the continental mantle lithosphere of stable North America. *Earth and Planetary Science Letters*, 425:12–23, 2015. doi: 10.1016/j.epsl.2015.05.048.

Craig, T., Copley, A., and Jackson, J. Thermal and tectonic consequences of India underthrusting Tibet. *Earth and Planetary Science Letters*, 353-354, 2012. doi: 10.1016/j.epsl.2012.07.010.

Craig, T., Kelemen, P., Hacker, B., and Copley, A. Reconciling geophysical and petrological estimates of the thermal structure of southern Tibet. *Geochemistry, Geophysics, Geosystems*, 21(8): e2019GC008837, 2020. doi: 10.1029/2019GC008837.

Craig, T., Jackson, J., Priestley, K., and Ekstrom, G. A Cautionary Tale: examples of the mis-location of small earthquake beneath the Tibetan plateau by routine approaches. *Geophysical Journal International*, 233, 2023. doi: 10.1093/gji/ggad025.

EarthScope Consortium. Global Seismograph Network — II. *International Federation of Digital Seismograph Networks*, 1986. doi: 10.7914/SN/II.

Federal Institute for Geosciences and Natural Resources (BGR). German Regional Seismic Network. *International Federation of Digital Seismograph Networks*, 1976. doi: 10.25928/mbx6-hr74.

Frohlich, C., Gan, W., and Herrmann, R. B. Two deep earthquakes in Wyoming. *Seismological Research Letters*, 86(3):810–818, 2015. doi: 10.1785/0220140197.

Hanan, B. B., Shervais, J. W., and Vetter, S. K. Yellowstone plume–continental lithosphere interaction beneath the Snake River Plain. *Geology*, 36(1):51–54, 2008. doi: 10.1130/G23935A.1.

Hutchings, S. J., Koper, K. D., Burlacu, R., Zeng, Q., Lin, F.-C., and Zandt, G. Upper mantle earthquakes along the edge of the Wyoming Craton. *Geophysical Research Letters*, 52(9): e2024GL114073, 2025. doi: 10.1029/2024GL114073.

Hutchings, S. J., Koper, K. D., and Pang, G. A seismically active shear zone in the uppermost mantle beneath the Canadian Rockies. *Geophysical Research Letters*, 53(1):e2025GL117818, 2026. doi: 10.1029/2025GL117818.

Idaho National Laboratory. INL Seismic Monitoring Program. *International Federation of Digital Seismograph Networks*, 1972. doi: 10.7914/SN/IE.

Institute of Geophysical Research (KNDC). Kazakhstan Network. *International Federation of Digital Seismograph Networks*, 1994. doi: 10.7914/SN/KZ.

Kind, R., Yuan, X., and Kumar, P. Seismic receiver functions and the lithosphere–asthenosphere boundary. *Tectonophysics*, 536: 25–43, 2012. doi: 10.1016/j.tecto.2012.03.005.

Koper, K. D., Hutchings, S. J., Burlacu, R., Whidden, K., Springer, V., Tibi, R., and Pang, G. The 10 September 2025 M w 4.1 Earthquake in Northeastern Utah, United States: An Archetypal Continental Mantle Event. *The Seismic Record*, 6(2):167–177, 2026. doi: 10.1785/0320260006.

Li, A. and Dave, R. Destroying a Craton by Plate Subduction, Small-scale Convection, and Mantle Plume: Comparison of the Wyoming Craton and the North China Craton. In *AGU Fall Meeting Abstracts*, volume 2016, pages T21F–02, 2016.

Lindenfeld, M. and Rümpker, G. Detection of mantle earthquakes beneath the East African Rift. *Geophysical Journal International*, 186(1):1–5, 2011. doi: 10.1016/j.tecto.2012.07.010.

McCafferty, A., San Juan, C., Lawley, C., Graham, G., Gadd, M., Huston, D., Kelley, K., Paradis, S., Peter, J., , and Czarnota, K. National-scale geophysical, geologic, and mineral resource data and grids for the United States, Canada, and Australia: Data in support of the tri-national Critical Minerals Mapping Initiative (ver 1.1, March 2025) [Data release], 2023. doi: 10.5066/P970GDD5.

Monsalve, G., Sheehan, A., Schulte-Pelkum, V., Rajaure, S., Pandey, M., and Wu, F. Seismicity and one-dimensional velocity structure of the Himalayan collision zone: Earthquakes in the crust and upper mantle. *Journal of Geophysical Research: Solid Earth*, 111(B10), 2006. doi: 10.1029/2005JB004062.

National Institute for Earth Physics (NIEP). Romanian Seismic Network. *International Federation of Digital Seismograph Networks*, 1994. doi: 10.7914/SN/RO.

Natural Resources Canada. Canadian National Seismograph Network. *International Federation of Digital Seismograph Networks*, 1975. doi: 10.7914/SN/CN.

NORSAR. NORSAR Station Network. *International Federation of Digital Seismograph Networks*, 1971. doi: 10.21348/d.no.0001.

Paul, H., Sunilkumar, T. C., Naresh, B., and Ravi Kumar, M. Minor Lithospheric Mantle Earthquakes Beneath the South Indian Shield: Implications for Continental Mantle Rheology. *Journal of Geophysical Research: Solid Earth*, 130(10):e2025JB031522, 2025. doi: 10.1029/2025JB031522.

Priestley, K., Jackson, J., and McKenzie, D. Lithospheric structure and deep earthquakes beneath India, the Himalaya and southern Tibet. *Geophysical Journal International*, 172(1):345–362, 2008. doi: 10.1111/j.1365-246X.2007.03636.x.

Prieto, G. A., Froment, B., Yu, C., Poli, P., and Abercrombie, R. Earthquake rupture below the brittle-ductile transition in continental lithospheric mantle. *Science Advances*, 3(3):e1602642, 2017. doi: 10.1126/sciadv.1602642.

Reyners, M., Eberhart-Phillips, D., and Stuart, G. The role of fluids in lower-crustal earthquakes near continental rifts. *Nature*, 446: 1075–1078, 2007. doi: 10.1038/nature05743.

Rigo, A., Adam, C., Grégoire, M., Gerbault, M., Meyer, R., Rabinowicz, M., Fontaine, F., and Bonvalot, S. Insights for the melt migration, the volcanic activity and the ultrafast lithosphere delamination related to the Yellowstone plume (Western USA). *Geophysical Journal International*, 203(2):1274–1301, 2015. doi: 10.1093/gji/ggv360.

Rost, S. and Thomas, C. Array seismology: Methods and applications. *Reviews of geophysics*, 40(3):2–1, 2002. doi: 10.1029/2000RG000100.

Schulte-Pelkum, V., Monsalve, G., Sheehan, A. F., Shearer, P., Wu, F., and Rajaure, S. Mantle earthquakes in the Himalayan collision zone. *Geology*, 47(9):815–819, 2019. doi: 10.1130/G46378.1.

Shen, W. and Ritzwoller, M. H. Crustal and uppermost mantle structure beneath the United States. *Journal of Geophysical Research: Solid Earth*, 121(6):4306–4342, 2016. doi: 10.1002/2016JB012887.

Shinevar, W. J., Jagoutz, O., and Behn, M. D. WISTFUL: Whole-rock interpretative seismic toolbox for ultramafic lithologies. *Geochemistry, Geophysics, Geosystems*, 23(8):e2022GC010329, 2022. doi: 10.1093/petrology/egy048.

Shinevar, W. J., Golos, E. M., Jagoutz, O., Behn, M. D., and Van der Hilst, R. D. Mantle thermochemical variations beneath the continental United States through petrologic interpretation of seismic tomography. *Earth and Planetary Science Letters*, 602: 117965, 2023. doi: 10.1016/j.epsl.2022.117965.

Sloan, R. and Jackson, J. Upper-mantle earthquakes beneath the Arafura Sea and south Aru Trough: Implications for continental rheology. *Journal of Geophysical Research: Solid Earth*, 117(B5), 2012. doi: 10.1029/2011JB008992.

Soosalu, H., Key, J., White, R., Knox, C., Einarsson, P., and Jakobsdóttir, S. Lower-crustal earthquakes caused by magme movement beneath Askja volcano on the north Iceland rift. *Bulletin of Volcanology*, 72, 2010. doi: 10.1007/s00445-009-0297-3.

Tape, W. and Tape, C. Angle between principal axis triples. *Geophysical Journal International*, 191(2):813–831, 2012. doi: 10.1111/j.1365-246X.2012.05658.x.

Thielmann, M. Grain size assisted thermal runaway as a nucleation mechanism for continental mantle earthquakes: Impact of complex rheologies. *Tectonophysics*, 746:611–623, 2018. doi: 10.1016/j.tecto.2017.08.038.

University of Utah. University of Utah Regional Seismic Network. *International Federation of Digital Seismograph Networks*, 1962. doi: 10.7914/SN/UU.

University of Utah. Yellowstone National Park Seismograph Network. *International Federation of Digital Seismograph Networks*, 1983. doi: 10.7914/SN/WY.

USGS. Advanced National Seismic System (ANSS) Comprehensive Catalog of Earthquake Events and Products [Data set], 2017. doi: 10.5066/F7MS3QZH.

Various Institutions. International Miscellaneous Stations. *International Federation of Digital Seismograph Networks*, 1965. doi: 10.7914/vefq-vh75.

Vasyura-Bathke, H., Dettmer, J., Steinberg, Andreasand Heimann, S., Isken, M., Zielke, O., Mai, P. M., Sudhaus, H., and Jónsson, S. BEAT - Bayesian Earthquake Analysis Tool. V. 1.0 [Software], 2019. doi: 10.5880/fidgeo.2019.024.

Woo, J.-U. and Chen, T. Mantle Earthquakes: Deep Quakes Beneath the Moho in the Wyoming Craton. *The Seismic Record*, 5 (4):363–373, 2025. doi: 10.1785/0320250032.

Xiao, H., Marshak, S., DeLucia, M., and Song, X. Moho depth (crustal thickness) variations under the northeastern midcontinent of North America, based on H-κ- c receiver-function analysis. *Earth and Planetary Science Letters*, 658:119289, 2025. doi: 10.1016/j.epsl.2025.119289.

Zandt, G. and Richins, W. An upper mantle earthquake beneath the middle Rocky Mountains in NE Utah. *Earthquake Notes*, 50 (4):69–70, 1979.

Zhang, H., Ravat, D., and Lowry, A. R. Crustal composition and Moho variations of the central and eastern United States: Improving resolution and geologic interpretation of EarthScope USArray seismic images using gravity. *Journal of Geophysical Research: Solid Earth*, 125(3):e2019JB018537, 2020. doi: 10.1029/2019JB018537.

Zhao, D., Liang, X., Toyokuni, G., Hua, Y., and Xu, Y.-G. Cause of enigmatic upper-mantle earthquakes in central Wyoming. *Seismological Research Letters*, 95(4):2497–2505, 2024. doi: 10.1785/0220230333.

The article *A rare earthquake in the upper mantle of subcontinental lithospheric mantle of North America* © 2026 by Benedict Fitton is licensed under CC BY 4.0.